Available online at www.sciencedirect.com
ScienceDirect
Journal of the European Ceramic Society 29 (2009) 3113–3119
www.elsevier.com/locate/jeurceramsoc

Direction dependent mechanical properties of extruded cordierite honeycombs

Conrad Bubeck *

Robert Bosch GmbH, Robert-Bosch-Platz 1, CR/ARM, 70839 Gerlingen, Germany

Received 3 October 2008; received in revised form 24 May 2009; accepted 10 June 2009
Available online 9 July 2009

Abstract

The description of the texture in an extruded honeycomb structure of cordierite and its effects on mechanical properties is the main goal of this paper. To understand the behaviour of the extruded material, the elastic properties of a natural cordierite single crystal with a transversal isotropic behaviour were determined with different methods. The CTE and Young's modulus in an extruded structure were empirically correlated with the preferred orientation of the grains and single crystal measurements. The correlated properties were compared with the measured properties. The Young's modulus shows a similar behaviour in different directions while the CTE shows a strong anisotropy, and it is thought that microcracking may influence both properties.

Keywords: Extrusion; X-ray methods; Mechanical properties; Silicate; Engine components

1. Introduction

The coefficient of thermal expansion (CTE) for the cordierite single crystal is negative in one direction. A crystal texture in a component will cause different CTEs in different directions. Cordierite is commonly used in the automotive industry for catalyst substrates and diesel particulate filters. It has been known for long that the CTE of extruded cordierite is extremely low and that cordierite has a robust thermal shock resistance. But the median CTE of the single crystal of cordierite[1] does not fit with measured CTEs of the extruded honeycomb structure in axial and radial direction. The extrusion of the honeycomb structure tends to produce a specific texture in the extruded walls. This work will give a more specific description of the orientation of the single crystals in an extruded cordierite honeycomb structure. The difference of the orientation in direction of extrusion and in the perpendicular direction will be described through XRD measurements at important areas in the structure. The properties of the single crystal and the orientation will help to understand the properties of the extruded honeycomb structure. The results of the single crystal were compared to the results of the component in respect to the orientation of the single crystals. Some samples of the extruded material were pressed to a solid material before sintering. The properties of this material were measured and discussed in respect to the measured properties of the square cell structure.

2. Experimental

2.1. CTE of cordierite

CTE was measured with a Netzsch Dilatometer 402C with fused silica rods (always measured during heating from 25 to 1000 °C). The honeycomb structure requires two different specimen geometries to describe the CTE of the structure. Two different specimen types are shown in Fig. 1. The axial specimen represents the direction of extrusion and the radial specimen describes the direction perpendicular to the direction of extrusion.

2.2. Young's modulus

2.2.1. Cordierite single crystal

To describe the direction dependent mechanical properties of the extruded honeycomb structure, the properties of the

* Correspondence address: Muelbergerstr. 60, 73728 Esslingen, Germany. Tel.: +49 711 9145140.
E-mail address: bubeck@gmx.de.

0955-2219/$ – see front matter © 2009 Elsevier Ltd. All rights reserved.
doi:10.1016/j.jeurceramsoc.2009.06.005

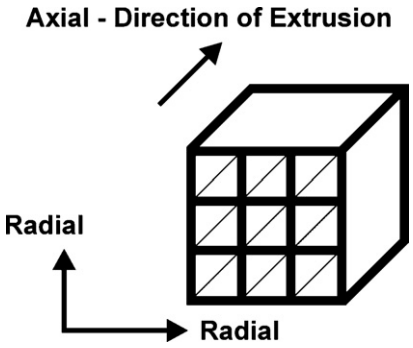

Fig. 1. Definition of the axial and radial direction in the square cell structure.

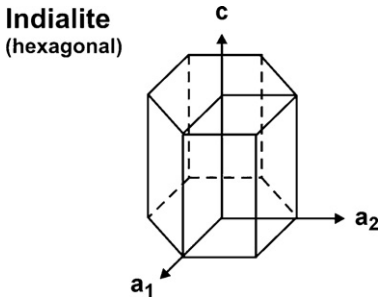

Fig. 2. Schematic graph of the hexagonal cordierite structure of the single crystal.

cordierite single crystal were of interest. To get the stiffness of the single crystal, a natural cordierite single crystal from South Africa was used. A cube with the size of 6.89 mm was prepared so that the *c*-axis of the single crystal overlapped with an axis of the cube. The natural cordierite shows similar weight components of SiO_2, Al_2O_3 and MgO in relation to the sintered cordierite, and is in accordance with the results of Toohill.[2] On the assumption of transversal isotropy along the *c*-axis, the stiffness matrix was measured with ultrasonic phase spectroscopy (UPS)[3] and resonant ultrasound phase spectroscopy (RUS)[4] at MaTeCon GmbH.[5] Fig. 2 shows the coordinate system of the cube of the cordierite single crystal. The *c*-axis of the single crystal is in the direction 3 of the coordinate system of the stiffness matrix. The geometric dimension and the weight of the single crystal cube are shown in Table 1. The stiffness matrix was deduced from the measurement of the velocity of sound with the UPS and RUS. With the UPS, the elastic constants C_{11}, C_{22}, C_{33}, C_{44}, C_{55} and C_{66} were determined. Each constant was averaged over at least 3 measurements. The constants were calculated from the velocities and the density of the cube. The other constants C_{12}, C_{13} and C_{23} were identified with RUS.

Table 1
Geometry and density of the cordierite cubes.

Sample	Mass (g)	L_1 (mm)	L_2 (mm)	L_3 (mm)	Density (g/cm^3)
Single crystal	0.8463	6.89	6.89	6.89	2.59
Pressed 90°	2.1694	11.07	11.40	11.08	1.55
Pressed 45°	1.1603	11.17	7.76	9.07	1.48

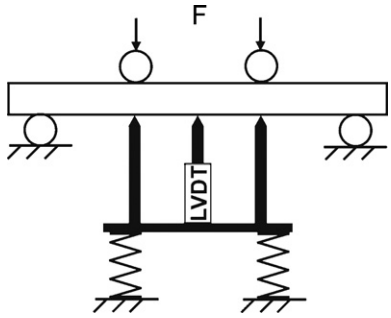

Fig. 3. Schematic graph of the measurement of the Young's modulus; a linear variable differential transformer (LVDT) is used for measuring the displacement of the specimen.

The natural vibrations of the specimen were activated in a frequency range from 100 kHz to 1 MHz. In this range 80, resonant frequencies were detected. With the measured frequencies the constants C_{12}, C_{23}, C_{33}, C_{44} and C_{66} were fitted (least square fit) iterative with the C-Code of Migliori and Sarro.[4]

2.2.2. Extruded cordierite with honeycomb structure

The Young's modulus was measured in a 4-Point-Bending-Test (4PB). A specimen with 4 cells vertical and 4 cells horizontal (4 × 4) and a length of 50 mm was bent in a 4PB. The deflection was measured at three different positions (in the middle of the specimen, under the inner rolls in the 4PB—Fig. 3) while the load was applied. With the applied moment and considering the accurate moment of inertia for the 4 × 4 specimen structure, the Young's modulus was calculated. Measurements (Young's modulus) in radial direction in the 4PB are not valid because the structure of the radial specimen deforms strongly and the measured bending does not only depend on the material property. A FEM (finite element method) simulation of a radial specimen in a 4PB showed a strong deformation of the square cell (square cell to rhombus) for the most part between the outer rolls. The result underestimates the Young's modulus in radial direction, because the measured deflection is too high and no accurate formulas for this structure are available to adjust the results.

2.2.3. Extruded cordierite—pressed before sintering

To get a better understanding of the properties, an extruded honeycomb structure was pressed to a solid (without square cells) in a green state before sintering. The extruded structure is shown in Fig. 4. The axis 3 in the extruded cell structure indicates the direction of extrusion. After the extrusion, the vertical walls were sheared in the 1–2-plane until the material was dense. After sintering, two pressed cubes were prepared to identify the stiffness matrix (Table 1). The first cube (pressed 90°) had the direction of extrusion in direction 3 of the stiffness matrix. The second cube (pressed 45°) had the direction of extrusion in 2–3-plane (direction 3, rotated about −45° around the axis 1). These cubes were also measured with the UPS and RUS method. With measurements on both cubes, the evaluation of the stiffness matrix is possible assuming a transversal isotropic behaviour along the direction of extrusion.

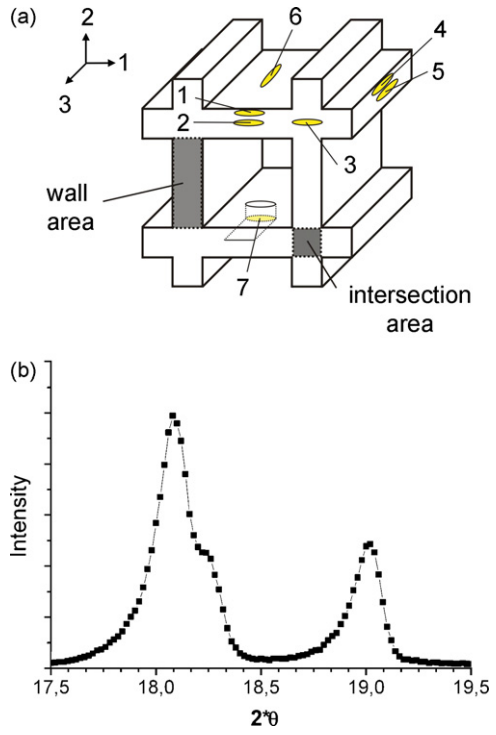

Fig. 4. (a) Positions of the different areas measured for the microdiffractometer to describe the orientation of the *c*-axis in the extruded honeycomb structure (the direction of the radiation is along the longer axis of the ellipse), cell wide $l_c = 1.1$ mm and wall thickness $l_w = 0.3$ mm. (b) X-ray diffraction diagram of position 2.

2.3. Distribution of the c-axis in a honeycomb structure

The orientation of the *c*-axis of the cordierite single crystals in an extruded honeycomb structure is described by Rasch[1] and Lachman.[6] Rasch showed a preferential orientation of the *c*-axis in the direction of extrusion (direction 3 in Fig. 4a). Lachman describes that the *c*-axis of the single crystals are in the plane of the extruded wall but without a preferential orientation. To describe the distribution of the *c*-axis in the extruded honeycomb, seven different interesting areas (Fig. 4a) were measured by XRD. The measurements were made with a Bruker-AXS D8advance Microdiffractometer (100 μm collimator and hi-star areal detector, Cu Kα radiation). For comparison, the *I*-ratio for non-oriented powder of the same material was measured with a Bruker-AXS D8advance Diffractometer (aperture stop 1 mm, Cu Kα radiation) with a powder-holder (side loading), where no force to the powder is applied. The degree of orientation was defined by an XRD intensity ratio (*I*-ratio)[6]:

$$I\text{-ratio} = \frac{I_{110}}{I_{110} + I_{002}} \quad (1)$$

The values of I_{110} and I_{002} represent the peak area (integrated intensity—peak function: Pearson VII) of the reflection from the planes (1 1 0) and (0 0 2) of the cordierite polycrystals. The plane (1 1 0) is parallel and (0 0 2) perpendicular to the *c*-axis. The reflection of the XRD plane (1 1 0) is at $2\theta = 18.14^\circ$ and the plane (0 0 2) at $2\theta = 18.95^\circ$ for Indialite. The lower the concentration of crystallite *c*-axis in the direction normal to the measured surface, the higher the *I*-ratio and vice-versa.

The relative peak areas are a function of the degree of a preferred orientation of the *c*-axis of the crystallites in the honeycomb structure. The results are estimated as from hexagonal cordierite (high form, Indialite). It is structurally similar to the orthorhombic cordierite (low form).[6] The extruded and normally sintered cordierite is a compound between the low form (orthorhombic) and the high form (hexagonal) with a specific characteristic. This can be observed in Fig. 4b. In the range of $2\theta = 18.14^\circ$ the peak shows a hump. This is caused by the fact that the low form cordierite has two peaks for plane (3 1 0) at $2\theta = 18.03^\circ$ and plane (0 2 0) at $2\theta = 18.21^\circ$ which are similar to plane (1 1 0) of Indialite, while plane (0 0 2) is at $2\theta = 19.00^\circ$ for the low form (similar to plane (0 0 2) of Indialite).

Different areas were measured to describe the orientation of the *c*-axis in the honeycomb structure (Fig. 4). Areas 1–3 are perpendicular to the direction of extrusion. In this plane, three areas are of major interest. Areas 1 and 2 describe the orientation in an extruded wall near the surface and in the center, area 3 in the intersection. Areas 4–7 are parallel to the direction of extrusion. Areas 4 and 5 describe the orientation in a wall near the surface and in the center. Area 6 describes the orientation on the surface of the extruded honeycomb structure while area 7 describes the orientation in the center of the wall, parallel to the surface. With the information of the *I*-ratios of the 7 areas and the information of a pure random orientation (non-orientated powder), a preferred distribution or orientation of the *c*-axis in the extruded square cell structure can be evaluated.

3. Results and discussion

3.1. CTE

The CTEs of the cordierite single crystal were measured by Fischer[7] and Ikawa[8] (Table 2). While Fischer presented only three values of the CTE, Ikawa measured the thermal expansion of high and low cordierite in the direction of different axes at many temperatures. Table 2 shows a profound difference of the CTE between the high form and the low form. While the expansion in the *a*-axis increased, the contraction in the *c*-axis increased too. Natural cordierite has usually the low form, while extruded and sintered square cell structures

Table 2
CTE measured by Fischer[8] and Ikawa[9].

	CTE (10^{-6}/K)
Fischer, 1974	
a_1–a_2-axis	$\alpha_{25\cdots1200} = 2.97$
c-axis	$\alpha_{25\cdots1200} = -0.77$
Ikawa, 1988	
High a_1–a_2-axis	$\alpha_{25\cdots1000} = 3.29$
High *c*-axis	$\alpha_{25\cdots1000} = -0.47$
Low *a*-axis	$\alpha_{25\cdots1000} = 4.26$
Low *b*-axis	$\alpha_{25\cdots1000} = 3.90$
Low *c*-axis	$\alpha_{25\cdots1000} = -0.89$

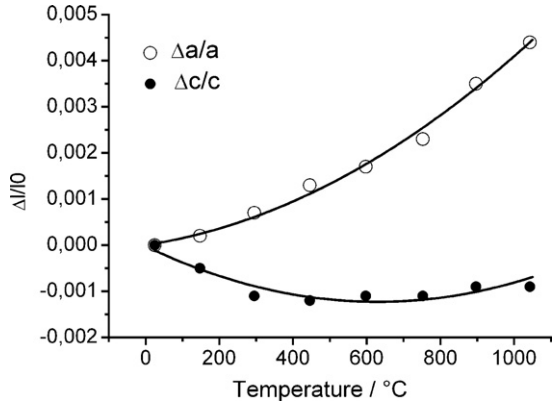

Fig. 5. Thermal expansion of hexagonal cordierite in the direction of the *a*-axis and *c*-axis.[9]

have the high form. Prolonged heating ($t > 100$ h at 1330 °C) showed a change by which the high form (hexagonal) is converted with time and temperature to the low form (orthorhombic) which is stable at that temperature.[9–11] To correlate the material behaviour of the extruded cordierite, the CTE of the single crystal with the high form in the direction of the *c*-axis is assumed to be $\alpha_c = -0.47\text{E}{-}06$ 1/K and in the direction of the *a*-axis $\alpha_a = 3.29\text{E}{-}06$ 1/K.[8] Fig. 5 shows the temperature dependent expansion of the *a*- and *c*-axes of the high form cordierite single crystal.

The measured extension and the CTE of the honeycomb structure are shown in Fig. 6 for the axial and radial direction. The results show a transversal isotropic behaviour in an extruded cordierite honeycomb structure. The CTE in axial direction is $\alpha_{ax} = 0.41\text{E}{-}06$ 1/K and in radial direction $\alpha_{\text{rad}} = 1.15\text{E}{-}06$ 1/K. In axial direction, the original length is reached at 705 °C and in radial direction at 220 °C. These results are between the expansion of the *a*-axis and the *c*-axis of the single crystal. This is caused by a preferential distribution of the single crystals in the extruded structure. The average value for the CTE of the extruded honeycomb structure is $\alpha_{\text{structure}} = 0.90\text{E}{-}06$ 1/K, while the average value for the single crystal is $\alpha_{\text{single}} = 2.04\text{E}{-}06$ 1/K (Table 2—Ikawas high cordierite). Therefore, there is a profound difference between the CTE of the single crystal and the extruded structure. This will be discussed in Section 3.4.

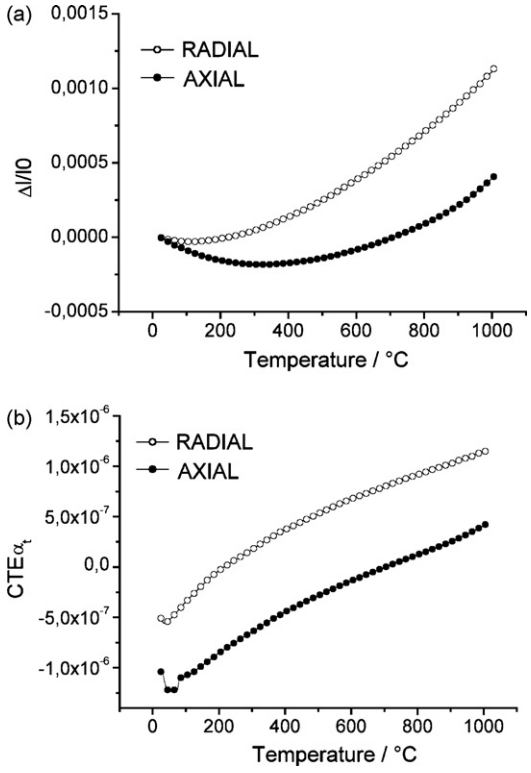

Fig. 6. Thermal expansion of the extruded cordierite honeycomb structure in axial and radial direction (a) change in length (b) the technical CTE relating to initial length at room temperature (25 °C).

Table 3
Results of the UPS and RUS of the cordierite single crystal.

	UPS (GPa)	RUS (GPa)
C_{11}	202.8	200.9
C_{12}	–	85.6
C_{13}	–	83.7
C_{22}	199.7	200.9
C_{23}	–	83.7
C_{33}	175.2	176.1
C_{44}	48.3	47.3
C_{55}	45.7	47.3
C_{66}	58.6	57.6

3.2. Young's modulus

The results for the material constants for the cordierite single crystal are shown in Table 3. The results of the UPS confirm the hypothesis of the transversal isotropy along the *c*-axis (3-axis) of the single crystal. The difference between the averages of C_{11} and C_{22} is 1.5%, whereas the difference to C_{33} is about 13%. Also the constants C_{44} and C_{55} have a difference of 2.7%, and C_{66} is about 25% higher.

To fit the constants of the stiffness matrix iteratively to the experimental resonance frequencies, the values of the UPS were used as starting values for the RUS fit to have fast convergence. With 78 natural measured frequencies, the constants C_{12}, C_{23}, C_{33}, C_{44} and C_{66} were fitted iteratively with the C-Code of Migliori and Sarro.[4] The assumption that C_{13} and C_{23} have the same value as C_{12} was made. For the values C_{11} and C_{22}, the average from the values C_{11} and C_{22} (UPS) was used. The same was done for C_{44} and C_{55}. The stiffness matrix and the Young's modulus show similar results as the cordierite of Toohill.[2] With the stiffness matrix the elastic constants were calculated[12] as presented in Table 4. The Young's modulus in the direction of the *a*-axis $E_a = 148.03$ GPa and in the direction of the *c*-axis

Table 4
Direction-dependent Young's modulus, shear-modulus and Poisson's ratio of the cordierite single-crystal.

	E_a (GPa)	E_c (GPa)	G_{ac} (GPa)	ν_{aa}	ν_{ac}
Single crystal	148.03	127.19	47.30	0.2844	0.3401

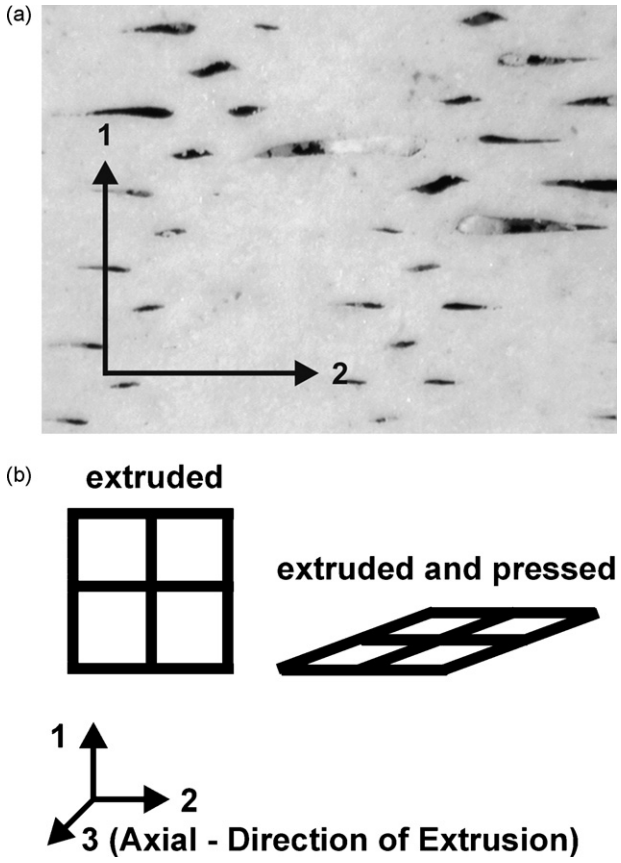

Fig. 7. (a) Extruded honeycomb structure pressed after extrusion—the honeycombs are incompletely pressed together, the direction of extrusion is perpendicular to the picture (b) Schematic of the pressed honeycomb structure.

$E_c = 127.19$ GPa. In the direction of the c-axis E has a 14% smaller value compared to the a-axis. This result can imply that a preferred orientation of the c-axis in a polycrystalline extruded structure produces a smaller Young's modulus in that direction.

To get the Young's modulus of the honeycomb structure in axial direction, each of the five specimens was loaded and unloaded four times. The average value of the measurements was taken for the Young's modulus of one specimen. Therefore, the Young's modulus was calculated as average value of the specimens to $E_{ax} = 9.40$ GPa for cordierite in the honeycomb structure in axial direction.

The geometric dimensions of the pressed cubes and their densities are shown in Table 1. The difference of the density indicates that the elastic properties of these cubes are not exactly the same. The pressed solid material shows flat void tubes in the cubes (Fig. 7).

Because of the asymmetric pressed square cells, an orthotropic symmetry was expected for the cubes. This results in an incomplete stiffness matrix with two cubes. Through a high weakening of the sound waves, the RUS-Method was not applicable on the extruded specimens. Therefore the results are from UPS. With additional tests on specimen "Pressed 45°", the constant C_{23} was calculated:

$$C_{23} = \sqrt{(C_{22} + C_{44} - 2 * \rho * \upsilon_{23/23}^2) * (C_{33} + C_{44} - 2 * \rho * \upsilon_{23/23}^2)} - C_{44} \quad (2)$$

Table 5
Results of the pressed square cell structure.

(GPa)	C_{11}	C_{22}	C_{33}	C_{44}	C_{55}	C_{66}
Pressed 90°	8.2	20.1	24.9	9.3	5.9	5.4

$\upsilon_{23/23}$ is a longitudinal wave, which spreads in direction 2 or 3 (Fig. 7). With UPS, the velocity was averaged over three measurements in both directions to $\upsilon_{23/23} = 4058$ m/s. For the density, the value of the specimen pressed 90° with 1.55 g/cm^3 was used. The constant C_{23} was calculated to $C_{23} = 9.8$ GPa. This result should be treated as an approximation because the assumption was made that both specimens have the same material behaviour. This assumption is not quite correct because there is a difference of 4.5% between the densities of the two cubes. This can cause an inexact stiffness matrix. The other constants are presented in Table 5. The highest value is the constant $C_{33} = 24.9$ GPa in the direction of extrusion and $C_{22} = 20.1$ GPa. $C_{11} = 8.2$ GPa is the lowest constant with a difference of 67% to the highest value. The highest value in the direction of extrusion means the highest stiffness in this direction. The constant of direction 2 of the pressed cube (Fig. 7b) represents the stiffness along the wall (perpendicular to area 5 in Fig. 4), while direction 1 shows the stiffness perpendicular to the wall (perpendicular to area 7 in Fig. 4). The directions 1 and 2 represent each a part of the stiffness in radial direction of the honeycomb structure while direction 3 represents the direction of extrusion. The results of the pressed cubes indicate that the stiffness in axial direction is higher than the stiffness in radial direction of the extruded honeycomb structure and a preferred orientation of the c-axis perpendicular to the direction of extrusion. With the stiffness of the single crystal (Table 4) and the results for the CTE (α_{ax}, α_{rad}) of the extruded honeycomb structure (Section 3.2), the stiffness matrix of the pressed cube indicates inconsistent behaviour. This is the result of the incompletely pressed solid cube from the honeycomb structure. The void tubes which are a result of the square cells of the extruded structure going continuously through the cube in direction 3 (Fig. 7). The ellipse form of these voids has a preferred orientation in direction 2. This produces a lower stiffness in direction 1. The same effect appears in direction 2 but is reduced because of the orientation of the ellipse voids.

3.3. Distribution of the c-axis in a honeycomb structure

The results of the different positions measured with XRD are shown in Table 6. The I-ratio for non-orientated cordierite is labeled Powder AM. Cordierite was ground in an agate mortar and measured in a powder-holder. Non-orientated cordierite has a measured I-ratio of 0.75. This value is different to the results measured by Lachman.[6] He measured an I-ratio = 0.65 for non-orientated cordierite made by isostatic pressing and an I-ratio = 0.63 for random powder. This effect is probably generated by the material and the different preparation methods of the powder. With the used powder holder (side loading), nearly no forces are applied to the powder.

Table 6
I-ratios at different areas and of the non-orientated powder.

	I-ratio
Area 1	0.35
Area 2	0.36
Area 3	0.55
Area 4	0.78
Area 5	0.73
Area 6	0.98
Area 7	0.86
Powder AM	0.75

Areas 1–3 (Fig. 4) show a clearly smaller coefficient than 0.75 which indicates a preferred orientation of the *c*-axis in the direction of extrusion in the wall and still a preferred orientation of the *c*-axis in the intersection in direction of extrusion. This fits with the hypothesis of Rasch.[1] Areas 4 and 5 show no significant differences to the non-oriented powder. Areas 6 and 7 show a higher *I*-ratio than the powder. The *I*-ratio of 0.98 on the surface of the extruded substrate indicates that near the surface, nearly all c-axes are lying parallel to the surface. The *I*-ratio of 0.86 indicates that in the middle of the wall, most *c*-axes are still lying in the plane parallel to the surface. The *I*-ratios of areas 1, 4 and 6 indicate a strong orientation in the direction of extrusion. Area 1 shows the lowest *I*-ratio. On area 6, nearly no intensity of (0 0 2) planes is detected. There are nearly no *c*-axes perpendicular to this surface. Therefore, the *I*-ratio of area 4 with the *I*-ratio of area 6 shows a preferred orientation of the *c*-axes in the direction of extrusion. An *I*-ratio of 0.75 does not necessarily predict that there is no orientation of the *c*-axes. The results of the areas 2, 5 and 7 in the center of the extruded channel walls give the same average *I*-ratio as the measurement near the surfaces of the walls (1, 4 and 6), but indicate a reduced orientation of the cordierite crystals.

3.4. Correlation of the properties of the single crystal and the polycrystal square cells

With the *I*-ratios of areas 1–7 and the CTEs of the single crystal (Table 2) it can be concluded that the CTE in the direction of extrusion is smaller than in the radial direction. The extruded honeycomb structure shows a preferred orientation of the *c*-axis in the direction of extrusion. However, a reason for a preferred growth of the *c*-axis in the disk shaped raw materials in the direction of extrusion is unknown. Lachman[6] noted that the material has a high expansion through the wall (perpendicular to area 6). That high expansion has no effect on the expansion of the structure. It should be noted that the average CTE of the extruded structure does not have the same value as the average CTE of the single crystal. At the interface in the radial direction between the wall and the intersection (areas 1–3) is the highest difference in the CTE in the direction of extrusion. This could result in increased thermal stresses in the surface between the wall and the intersection.

The CTE of the extruded honeycombs depend on the orientation of the single crystals in the extruded honeycomb structure. Now the behaviour of the square cell structure will be correlated with the orientation and the properties of the single crystal with

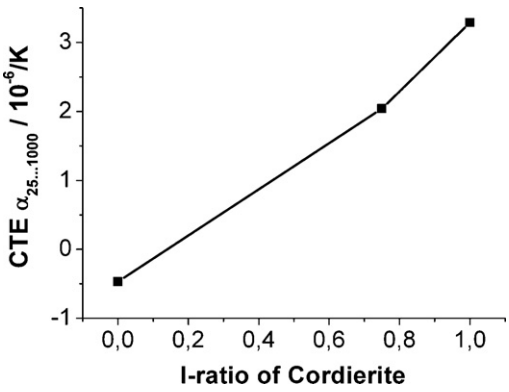

Fig. 8. CTE vs. *I*-ratio.

$\alpha_c = -0.47\text{E}{-}06$ 1/K and $\alpha_a = 3.29\text{E}{-}06$ 1/K[8] (see Section 3.1). Three correlations of the *I*-ratio and the CTE are known. For an *I*-ratio of 0, a CTE of $\alpha_c = -0.47\text{E}{-}06$ 1/K is expected in the direction perpendicular to the area measured by XRD. For an *I*-ratio of 0.75, an average CTE of $\alpha_{av} = 2.04\text{E}{-}06$ 1/K and for an *I*-ratio of 1 an CTE of $\alpha = 3.29\text{E}{-}06$ 1/K. A linear correlation between these points was assumed as an approximation (Fig. 8). For the correlation of the CTE in axial direction (Eq. (3)) it was assumed that the CTE can be calculated by an average CTE of the initial cell in the direction perpendicular to areas 1–3. Areas 1 and 2 were represented each with a wall area and area 3 by the intersection area (see Fig. 4)

$$\alpha_{\text{axial\_calc}} = \frac{\alpha_{I\text{-ratio\_}a1} * 1.1 + \alpha_{I\text{-ratio\_}a2} * 1.1 + \alpha_{I\text{-ratio\_}a3} * 0.3}{2 * 1.1 + 0.3} \quad (3)$$

For the correlation of the CTE in radial direction (Eq. (4)) it was assumed that the CTE was calculated by a weighted sum for CTEs in a direction perpendicular to areas 4, 5 and an area for the intersection represented by an assumed *I*-ratio of 0.82 (Fig. 8)

$$\alpha_{\text{radial\_calc}} = \frac{\alpha_{I\text{-ratio\_}a4} * (1.1/2) + \alpha_{I\text{-ratio\_}a5} * (1.1/2) + \alpha_{I\text{-ratio\_}0.82} * (0.3)}{0.3 + 1.1} \quad (4)$$

The correlated and the measured CTEs in axial and radial directions are presented in Table 7. The CTE in radial direction is higher than the CTE in axial direction. The correlated CTEs are approximately two times higher than the measured ones. A change of the calculation principle will have an effect on the correlated CTE. But with a minimum *I*-ratio of 0.35, the minimum possible CTE of $\alpha = 0.70\text{E}{-}06$ 1/K is still larger as the measured CTE ($\alpha_{\text{radial}} = 0.41\text{E}{-}06$ 1/K). Thus, the orientation of the single crystals cannot describe the CTE of the material

Table 7
CTE of the cordierite in honeycomb structure.

	Axial	Radial
Measured CTE (10^{-6}/K)	0.41	1.15
Correlated CTE (10^{-6}/K)	0.80	2.14

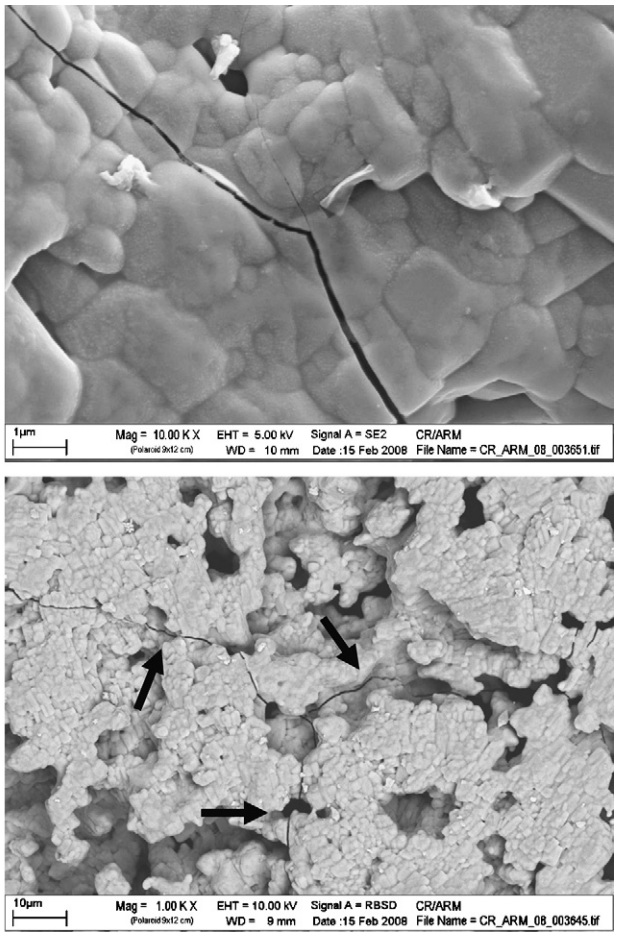

Fig. 9. (a) SEM picture (×10,000) of the surface of cordierite with microcracks (b) SEM picture (×1000) of the surface of cordierite with microcracks (black arrows).

sufficiently. There are other factors in the material (e.g. grain boundaries, microcracks) which have an influence on the CTE. A high density of microcracks (Fig. 9) at the surface and in the porous structure can cause a smaller CTE and explain a part of the difference between the measured and the correlated CTE (Table 7). These microcracks occur during the cool down of the sintered body preferentially at points with a high gradient of the CTEs to reduce internal stresses.

Another interesting relation is the ratio $\alpha_{radial}/\alpha_{axial}$ (Table 7). For the measured and for the correlated CTEs the ratio is approximately 2.7. That shows an equal effect of the microcracks for axial and radial direction. A preferred orientation of the microcracks would show a different value.

The Young's modulus of the single crystal has, in contrast to the CTE, only a difference of 14% between the axial and radial directions. With the results of Section 3.3 (a preferred orientation in the extruded structure) it can be concluded that the Young's modulus in the direction of extrusion is smaller than in radial direction. This result is important because the Young's modulus cannot be measured in the same way like in axial direction. An exact determination of the Young's modulus in radial direction is not possible, but the upper limit can be set with the axial value plus the difference of 14% to $E_{rad\_max} = 10.7$ GPa. The strong difference of the stiffness between the single crystal and the honeycomb structure is the result of porosity, microcracks and grain boundaries.

3.5. Conclusion

XRD-measurements at different areas in an extruded square cell structure of cordierite showed a preferred orientation of the *c*-axis of cordierite crystals parallel to the direction of extrusion. This confirms the hypothesis of Rasch.[1]

The distribution of the single crystals has a profound influence on the CTE. Microcracks decrease the thermal expansion of cordierite and show the same effect in axial and radial direction. A possible maximum effect is limited by the difference between the correlated and measured CTEs (approximately times 2 from 25 to 1000 °C—Table 7).

The Young's modulus of a single crystal of cordierite displays a difference of 14% between the *a*-axis and *c*-axis. The difference in stiffness in different directions by a preferred orientation of the single crystals is marginal in comparison to the CTE, pressed specimens with void tubes did not generate valid results from UPS measurements.

Acknowledgements

The author wishes to thank his colleagues at Robert Bosch GmbH for their assistance during this project, especially Dr. Martin Selten, Nicolas Maier and Dr. Thomas Köhler.

References

1. Rasch, H., Kapitel 4.1.3.0 Cordieritkeramik, Silicatkeramische technische Keramiken. *Handbuch der Keramik*, 1992, 1–55.
2. Toohill, K., Siegesmund, S. and Bass, J. D., Sound velocities and elasticity of cordierite and implications for deep crystal seismic anisotropy. *Phys. Chem. Miner.*, 1999, **26**, 333–343.
3. Wanner, A., Elastic modulus measurements of extremely porous ceramic materials by ultrasonic phase spectroscopy. *Mater. Sci. Eng.*, 1998, **A248**, 35–43.
4. Migliori, A. and Sarro, J. L., *Resonant Ultrasound Spectroscopy*. John Wiley and Sons, Inc, 1997, ISBN 0471123609.
5. A. Wanner, MaTeCon GmbH Materials Technology and Consulting, Bericht Nr. A070901 über ultraschallspektroskopische Untersuchungen an drei Cordierit-Proben (2007).
6. Lachman, I. M., Bagley, R. D. and Lewis, R. M., Thermal expansion of extruded cordierite ceramics. *J. Am. Ceram. Soc.*, 1981, **60**(2), S.202–S.205.
7. Fischer, G. R., Evans, D. L. and Geiger, J. E., B18 Crystal lattice thermal expansion of cordierite ($2MgO\ 2Al_2O_3\ 5SiO_2$) between RT and 1200 °C, presented at the American Crystallographic Association Summer Meeting at Pennsylvania State University, August 1974.
8. Ikawa, H., Ushimaru, Y., Urabe, K. and Udagawa, S., Axial thermal expansion of high and low cordierite and its solid solution. *Sci. Ceram.*, 1987, **14**, 769–774.
9. Winterstein, G., Mürbe, J. and Tupaika, F., Polymorphie von Cordierite in natürlichen Mineralien und in Cordieritwerkstoffen. *Keramische Zeitschrift*, 2003, **55**, 160–165.
10. Sorrell, C. A., Reaction sequence and structural changes in cordierite refractories. *J. Am. Ceram. Soc.*, 1960, **43**(7), 337–343.
11. Gibbs, G. V., The polymorphism of cordierite I: the crystal structure of low cordierite. *Am. Mineral.*, 1966, **51**(July).
12. Roesler, J., Harders, H. and Baker, M., *Mechanisches Verhalten der Werkstoffe*. Teubner Verlag, Wiesbaden, 2006, ISBN: 3835100084.